



1 **Improved identification of primary biological aerosol**
2 **particles using single particle mass spectrometry**

3

4 **Maria A. Zawadowicz¹, Karl D. Froyd^{2,3}, Daniel M. Murphy², and Daniel J.**
5 **Cziczo^{1,4}**

6 [1]{Department of Earth, Atmospheric and Planetary Sciences, Massachusetts Institute of
7 Technology, Cambridge, Massachusetts}

8 [2]{NOAA Chemical Sciences Division, Boulder, Colorado}

9 [3]{Cooperative Institute for Research in Environmental Sciences, University of Colorado,
10 Boulder, Colorado}

11 [4]{Department of Civil and Environmental Engineering, Massachusetts Institute of
12 Technology, Cambridge, MA, United States}

13 Correspondence to: D. J. Cziczo (djciczo@mit.edu)

14

15 **Abstract**

16 Measurements of primary biological aerosol particles, especially at altitudes relevant to cloud
17 formation, are scarce. Single particle mass spectrometry (SPMS) has been used to probe
18 aerosol chemical composition from ground and aircraft for over 20 years. Here we develop a
19 method for identifying bioaerosols using SPMS. We show that identification of bioaerosol
20 using SPMS is complicated because phosphorus-bearing mineral dust and phosphorus-rich
21 combustion by-products such as fly ash produce mass spectra with peaks similar to those
22 typically used as markers for bioaerosol. We have developed a methodology to differentiate
23 and identify bioaerosol using machine learning statistical techniques applied to mass spectra
24 of known particle types. This improved method provides far fewer false positives compared to
25 approaches reported in the literature. The new method was then applied to ambient data
26 collected at Storm Peak Laboratory to show that 0.04-0.3% of particles in the 200 – 3000 nm
27 aerodynamic diameter range were identified as bioaerosol.

28



1 **1 Introduction**

2 Primary biological aerosol, hereafter “bioaerosol”, include intact and fragmentary microbes,
3 fungal spores and vegetation. One particularly important role of bioaerosol in the atmosphere
4 is that certain species of bacteria and plant material might impact climate via the nucleation of
5 ice in clouds (Hiranuma et al., 2015; Möhler et al., 2008). However, field-based
6 measurements of ice nuclei and ice residuals do not indicate that bioaerosol are a major class
7 of ice active particles (Cziczo et al., 2013; DeMott et al., 2003; Ebert et al., 2011).
8 Uncertainties continue to exist because field measurements of ice nucleating particles are
9 currently sparse. Modeling efforts also suggest that biological material is not significant in ice
10 cloud formation on a global scale. Hoose et al. (2010) has shown that global average
11 contribution of bioaerosol to heterogeneous ice nucleation in mixed phase clouds is small:
12 with higher than realistic freezing efficiencies, the total contribution of biological aerosol
13 remained less than 1%. Later studies by Burrows et al. (2013), Sesartic et al. (2012, 2013) and
14 Spracklen and Heald (2014) support this result. These studies do identify circumstances
15 where bioaerosol can have an influence on clouds. For example, at low altitudes bacteria can
16 dominate immersion freezing rates, where the conditions are too warm for mineral dust to
17 activate ($>15^{\circ}\text{C}$) (Spracklen and Heald, 2014). Additionally, bioaerosol can dominate the
18 aerosol coarse modes in certain regions. For example bioaerosol can be 50% of the coarse
19 mode over tropical forests compared to a 5-8% global average (Spracklen and Heald, 2014).
20 There are measurements of this enhancement in the Amazon basin, supporting possible
21 regional effects of bioaerosol (Artaxo et al., 1990; Prenni et al., 2009).

22 Measurement techniques specific to bioaerosol include collection of aerosol on filters
23 followed by analysis with microscopy techniques, either electron microscopy (EM) or optical
24 microscopy coupled with fluorescent staining of the samples (Amato et al., 2005; Bauer et al.,
25 2002, 2008; Bowers et al., 2009, 2011, 2012; Griffin et al., 2001; Matthias-Maser and
26 Jaenicke, 1994; Pósfai et al., 2003a; Sattler et al., 2001; Wiedinmyer et al., 2009; Xia et al.,
27 2013). Aerosol samples collected in the atmosphere have been cultured for identification of
28 the microbial strains present (Amato et al., 2005, 2007; Fahlgren et al., 2010; Fang et al.,
29 2007; Griffin et al., 2001, 2006; Prospero et al., 2005). However, culturing techniques can
30 underestimate microbial diversity, as not all organisms present in the atmosphere are viable or
31 cultivable using standard media. It has been suggested that $<10\%$ of bacteria found in
32 atmospheric aerosol are cultivable (Amato et al., 2005; Georgakopoulos et al., 2009).



1 In-situ techniques specific to biological samples are typically based on fluorescence of
2 biological material following UV excitation. Examples include the wide-band integrated
3 bioaerosol sensor (WIBS) which is available commercially (Kaye et al., 2000, 2005). WIBS
4 has been successfully deployed in several locations (Gabey et al., 2010; O'Connor et al.,
5 2014; Toprak and Schnaiter, 2013). Using fluorescence to detect biological aerosol can have
6 interferences, however. For example, polycyclic aromatic compounds or humic acids can
7 have similar fluorescent properties (Gabey et al., 2010; Pan et al., 1999). Cigarette smoke has
8 similar fluorescent properties to bacteria (Hill et al., 1999). In an attempt to address
9 interferences, WIBS collects fluorescence information using several channels with different
10 wavelengths while also measuring the size and shape of the particles.

11 Table 1 summarizes recent measurements of bioaerosol in the atmosphere. Apart from WIBS,
12 the other recent measurements are collection of the aerosol on filters followed by off-line
13 microscopy. Biological particles have been measured at variety of ground sites, including
14 urban (Bauer et al., 2008; Fang et al., 2007; Toprak and Schnaiter, 2013), rural (Bowers et al.,
15 2011; Harrison et al., 2005), forest (Gabey et al., 2010), marine (Griffin et al., 2001; Pósfai et
16 al., 2003a) and remote (Xia et al., 2013). High-altitude mountain sites, such as Jungfraujoch,
17 Storm Peak Laboratory, Mt. Rax and Mt. Bachelor Observatory are often used to gain access
18 to free tropospheric air less impacted by local sources (Bauer et al., 2002; Bowers et al., 2012;
19 Smith et al., 2012, 2013; Wiedinmyer et al., 2009; Xia et al., 2013). Measured concentrations
20 range from 2.9×10^3 to 1.5×10^6 particles m^{-3} , and bioaerosol can make up from 0.5% to 22% of
21 atmospheric aerosol by number greater than 500 nm. There is a strong seasonal cycle to
22 biological material (Bowers et al., 2012; Harrison et al., 2005; Toprak and Schnaiter, 2013).
23 Bioaerosol tend to be primarily bacteria and some fungal spores, although pollen (O'Connor
24 et al., 2014) and possibly viruses (Griffin et al., 2001) have been reported. Some studies have
25 performed DNA analysis of bioaerosol, reporting a wide diversity (Smith et al., 2012, 2013;
26 Xia et al., 2015).

27 Bioaerosol has also been reported in cloud water (Amato et al., 2005; Bauer et al., 2002;
28 Sattler et al., 2001) and precipitation samples (Bauer et al., 2002; Christner et al., 2008a,
29 2008b; Sattler et al., 2001). This does not necessarily mean the bioaerosol play a role in
30 droplet nucleation processes, however, as scavenging of interstitial aerosol happens frequently
31 in and below clouds (Pruppacher and Klett, 2003). It does illustrate that microorganisms,



1 sometimes viable ones, can be transported by the atmosphere and deposited by precipitation
2 (Amato et al., 2005).

3 Measurements of bioaerosol in the free and upper troposphere, where they could be relevant
4 to cloud formation, remain scarce. Four of the recent studies reported in Table 1 used an
5 aircraft to access altitudes higher than 4,000 m (DeLeon-Rodriguez et al., 2013; Pósfai et al.,
6 2003a; Twohy et al., 2016; Ziemba et al., 2016). Two of these used the WIBS sensor to report
7 vertical profiles of fluorescent particles (Twohy et al., 2016; Ziemba et al., 2016). In the
8 remaining two cases, aerosols were collected on filters and analyzed off-line. Pósfai (2003a)
9 reported results of Transmission EM (TEM) measurements of samples collected around Cape
10 Grim that included bacteria with rod-like morphology. It should be noted that numerous other
11 studies of samples collected on aircraft missions with TEM microscopy did not reveal the
12 presence of any aerosols that matched morphology of biological material (Buseck and Pósfai,
13 1999; Li et al., 2003a, 2003b; Pósfai et al., 1994, 1995, 2003b). There can exist significant
14 uncertainty in these measurements. A recent aircraft-based study by DeLeon-Rodriguez et al.
15 (2013) reports analysis of high altitude (8-15 km) samples taken before, after and during two
16 major tropical hurricanes. The abundances of microbes, mostly bacteria, were reported
17 between 3.6×10^4 and 3.0×10^5 particles m^{-3} in the 0.25 – 1 μm size range. The methods and
18 conclusions of this study were re-evaluated by Smith and Griffin (2013), who argued that in
19 some instances the reported concentration of bioaerosol were not possible because they
20 exceeded the total aerosol by several factors. The samples were also taken over periods of
21 hours, possibly including sampling in clouds when the high-speed impaction of droplets and
22 ice can dislodge particles from the inlet (Cziczo and Froyd, 2014; Froyd et al., 2010; Murphy
23 et al., 2004).

24 Although difficult, measurements of bioaerosol in the upper troposphere are necessary in
25 order to constrain their influence on atmospheric properties and cloud formation processes.
26 All of the techniques discussed above, except for WIBS, are off-line and require expertise in
27 sample processing and decontamination. WIBS is a possible in situ detection technique for
28 bioaerosols, but it is relatively new and, as a result, has a short deployment history. There has
29 been considerable interest in using aerosol mass spectrometry techniques to measure
30 bioaerosol. Single particle mass spectrometry (SPMS) has been successfully used since the
31 mid-1990s to characterize chemical composition of atmospheric aerosol particles in situ and
32 in real time (Murphy, 2007). The ability of SPMS to simultaneously characterize volatile and



1 refractory aerosol components makes it an attractive tool for investigating the mechanisms of
2 cloud formation (Cziczo et al., 2013; Friedman et al., 2013). The general principle behind
3 SPMS, and in particular the instrument discussed in this paper, the Particle Analysis by Laser
4 Mass Spectrometry (PALMS), is the use of a pulsed UV laser for the ablation and ionization
5 of single aerosol particles. Ions are then accelerated into a time-of-flight mass spectrometer.
6 Laser ablation/ionization used with SPMS produces ion fragments and clusters and is
7 susceptible to matrix effects such that quantitative results are possible only with careful
8 calibration and consistent composition (Cziczo et al., 2001).

9 Biological aerosols have been studied with SPMS, in particular the Aerosol Time of Flight
10 Mass Spectrometer (ATOFMS; Cahill et al., 2015; Creamean et al., 2013; Fergenson et al.,
11 2004; Pratt et al., 2009). A property of SPMS bioaerosol spectra that has been exploited for
12 their detection is the presence of phosphate (PO^+ , PO_2^- , PO_3^-) and organic nitrogen ions (CN^- ,
13 CNO^-) (Cahill et al., 2015; Fergenson et al., 2004). Those ions have also been shown to be
14 present in non-biological particles with the same instrument, however, such as vehicular
15 exhaust (Sodeman et al., 2005). One goal of this work is to examine the prevalence of these
16 ions in the context spectra collected with other SPMSs.

17 Phosphorus is a limiting nutrient in terrestrial ecosystems (Brahney et al., 2015). On the
18 global scale, phosphorus-containing dust aerosols are primarily responsible for delivering this
19 nutrient to oceans and other ecosystems (Mahowald et al., 2008, 2005). Bioaerosols can be an
20 important source of atmospheric phosphorus on local scales, especially in heavily forested
21 areas, like the Amazon (Mahowald et al., 2005). The global phosphorus budget has been
22 modeled by Mahowald et al. (2008), indicating that 82% of the total burden is emitted in the
23 form of mineral dust. Bioaerosol accounts for 12% and anthropogenic combustion sources,
24 including fossil fuels, biofuels and biomass burning, account for 5% (Mahowald et al., 2008).
25 Recently, Wang et al. (2014) provided a higher estimate of phosphorus emissions from
26 anthropogenic combustion sources, 31%. In this estimate, mineral dust was responsible for
27 27%, bioaerosol 17% and natural combustion sources 20% of total phosphorus emissions
28 (Wang et al., 2014). These examples illustrate the major factors in the global phosphorous
29 budget but also that significant uncertainties exist in the emission inventories. A second goal
30 of this work is to determine if the non-biological phosphate aerosols, such as those from
31 minerals and combustion, can be detected and differentiated from bioaerosol.



1 **2 Experimental**

2 2.1 PALMS

3 The objective of this work is to describe and validate a new SPMS-based data analysis
4 technique that allows for the selective measurement of bioaerosol. A dataset of bioaerosol,
5 phosphate-rich mineral and coal fly ash single particle spectra – the three largest sources of
6 phosphorous in atmospheric aerosols - was used to derive a classification algorithm for
7 biological and non-biological phosphate-containing material. This classifier was then applied
8 to an ambient data set collected at the Storm Peak Laboratory during the Fifth Ice Nucleation
9 workshop—phase 3 (FIN03).

10 The NOAA PALMS instrument has been discussed in detail elsewhere (Cziczo et al., 2006;
11 Thomson et al., 2000). Currently, there are two copies of the PALMS instrument, both of
12 which were used in this work. The laboratory PALMS is a prototype for the flight PALMS,
13 which is more compact and can be deployed unattended at field sites and on aircraft
14 (Thomson et al., 2000). Briefly, PALMS uses an aerodynamic lens to sample aerosols and
15 impart them with a size-dependent velocity (Zhang et al., 2002, 2004). Aerodynamic particle
16 diameter is measured by timing the particles between two continuous-wave laser beams (532
17 nm Nd:YAG in laboratory PALMS and 405 nm diode in flight PALMS). The particles are
18 ablated and ionized in one step by a 193 nm excimer laser. A unipolar reflectron time of flight
19 mass spectrometer is then used to acquire mass spectra. Due to the high laser fluence used for
20 desorption and ionization ($\sim 10^9$ W/cm²), PALMS spectra show both atomic ions and ion
21 clusters, which complicate spectral interpretation. SPMS is considered a semi-quantitative
22 technique because the ion signal depends on the abundance and ionization potential of the
23 substance, rather than solely its abundance (Murphy, 2007). Additionally, the ion signals can
24 depend on the overall chemical composition of the particle, known as matrix effects (Murphy,
25 2007). The lower particle size threshold for PALMS is ~ 200 nm diameter and is set by the
26 amount of detectable scattered light. The upper size threshold is set by transmission in the
27 aerodynamic lens at ~ 3 μ m diameter (Cziczo et al., 2006). The 193 nm excimer laser can
28 ionize all atmospherically-relevant particles within this size range with little detection bias
29 (Murphy, 2007). The ionization region is identical in the laboratory and flight PALMS
30 instruments.

31 2.2 Test samples



1 A collection of phosphorus-containing samples of biological and inorganic origin were used
2 for this work. Some of the samples were analyzed with the laboratory PALMS at the Aerosol
3 Interaction and Dynamics in the Atmosphere (AIDA) facility at Karlsruhe Institute of
4 Technology (KIT) during the Fifth International Ice Nucleation Workshop—phase 1 (FIN01)
5 with the remainder sampled at MIT.

6 Biological aerosol sampled at AIDA included two aerosolized cultures of *Pseudomonas*
7 *syringae* bacteria, Snomax (Snomax International, Denver, CO) (irradiated, desiccated and
8 ground *Pseudomonas syringae*) and hazelnut pollen wash water. The Snowmax and *P.*
9 *syringae* cultures were suspended in water and aerosolized with a Collision-type atomizer. The
10 growth medium for *P. syringae* cultures was Pseudomonas Agar Base (CM0559, Oxoid
11 Microbiology Products, Hampshire, UK).

12 Biological aerosol sampled at MIT included giant ragweed (*Ambrosia trifida*) pollen, oak
13 (*Quercus rubra*) pollen, European white birch (*Betula pendula*) pollen, *Fusarium solani*
14 spores and yeast. Samples of dried pollens and *F. solani* spores were purchased from Greer
15 (Lenoir, NC). Information supplied by the manufacturer indicates that *F. solani* fungus was
16 grown on enriched trypticase growth medium and killed with acetone prior to harvesting the
17 spores. Ragweed and oak pollen originated from wild plants, while the birch pollen originated
18 from a cultivated plant. Pollen was collected, mechanically sieved and dried. The yeast used
19 in this experiment was commercial active dry yeast (Star Market brand). The yeast powder
20 was sampled by PALMS from a vial subjected to slight manual agitation. Pollen grains were
21 too large (18.9 – 37.9 μm according to manufacturer's specification) to sample with PALMS.
22 They were suspended in Milli-Q water (18.2 M Ω cm, Millipore, Bedford, MA) and the
23 suspensions were sonicated in ultrasonic bath for ~30 minutes to break up the grains. Large
24 material was allowed to settle to the bottom and a few drops of the clear solution from the top
25 of the suspensions were further dissolved in ~5 mL of Milli-Q water, and the resulting
26 solutions were aerosolized with a disposable medical nebulizer (Briggs Healthcare,
27 Waukegan, IL). A diffusion dryer was used to remove condensed phase water prior to
28 sampling with PALMS. *F. solani* spores were sampled in two different ways: (1) dry and
29 unprocessed, in the same way as the yeast and (2) fragmented in ultrasonic bath and wet-
30 generated, in the same way as pollen samples. No processing-related changes to chemistry
31 were found.



1 Internally mixed biological/mineral particles were also analyzed at MIT. Illite NX (Clay
2 Mineral Society) without bioaerosol was sampled dry, using a shaker (Garimella et al., 2014),
3 and wet-generated, using a medical nebulizer containing Milli-Q water. A second disposable
4 medical nebulizer was then used to aerosolize a solution of illite NX and *F. solani* spores.
5 This wet generated aerosol was also dried with a diffusion dryer prior to PALMS sampling.

6 Samples of fly ash from four coal-fired U.S. power plants were used as proxy for combustion
7 aerosol: J. Robert Welsh Power Plant (Mount Pleasant, TX), Joppa Power Station (Joppa, IL),
8 Clifty Creek Power Plant (Madison, IN) and Miami Fort Generating Station (Miami Fort,
9 OH). The samples were obtained from a commercial fly ash supplier, Fly Ash Direct
10 (Cincinnati, OH). Fly ash was dry generated with the shaker.

11 Apatite and Monazite-Ce mineral samples were generated from ~3” pieces of rock. The rocks
12 were ground and the samples aerosolized with the shaker. Both apatite and monazite were
13 sampled and processed at MIT. The apatite rock was contributed by Adam Sarafian (Woods
14 Hole Oceanographic Institution, Woods Hole, MA).

15 Samples of apatite and J. Robert Welsh Power Plant fly ash were also subjected to processing
16 with nitric acid to approximate atmospheric aging. Powdered sample was aerosolized from
17 the shaker to fill a 9 L glass mixing volume. A hot plate below the volume was used to heat
18 the air inside to 31°C measured in the center of the volume with a thermocouple. PALMS
19 sampled at a flow of 0.44 slpm from the 9 L volume. This constituted unprocessed aerosol.
20 80% HNO₃ was then placed with a Pasteur pipette at the heated bottom of the mixing volume.
21 Two experiments were conducted.: for 0.1 mL experiments the entire volume of HNO₃
22 evaporated, producing an estimated partial pressure of about 0.005 atm in a static situation. In
23 1 mL experiments some liquid HNO₃ remained at the bottom of the volume with an estimated
24 partial pressure of HNO₃ of 0.04 atm. The aerosol and gas-phase HNO₃ were allowed to
25 interact for 2 minutes at which point PALMS began sampling from the volume.

26 Samples of natural soil dust were collected from various locations listed in Table 2. Five
27 sampled were investigated at the AIDA facility during FIN01 (Bächli soil, Argentina soil,
28 Ethiopian soil, Moroccan soil and Chinese soil) with the remaining analysis at MIT (Storm
29 Peak and Saudi Arabian soil). Two samples of German soil were used as an example of
30 agricultural soil that was known to be fertilized with inorganic phosphate. These were also
31 sampled at the AIDA facility during FIN01.

32



1 2.3 Statistical analysis

2 A support vector machine (SVM), a supervised machine learning algorithm (Cortes and
3 Vapnik, 1995), was used as the statistical analysis method for analysis of these data. A portion
4 of the data from each of the bioaerosol and non-biological phosphate samples was used as
5 “training data” to build the algorithm. The remaining data were differentiated by the trained
6 algorithm and the correctness judged based on their source. In this case a non-linear binary
7 classifier was constructed, using non-linear kernel functions (Ben-Hur et al., 2001; Cortes and
8 Vapnik, 1995). A Gaussian radial basis function kernel was empirically determined to provide
9 the best performance in this case. For this work, the SVM algorithm was implemented in
10 MATLAB 2016a (MathWorks, Natick, MA) using the Statistics and Machine Learning
11 toolbox.

12 2.4 Field data

13 The method was employed on an ambient data set acquired at the Desert Research Institute’s
14 (DRI’s) Storm Peak Laboratory located in Steamboat Springs, CO. Storm Peak Laboratory is
15 located on Mt. Werner at 3220 m elevation at 106.74 W, 40.45 N. This high altitude site is
16 often in free tropospheric air, mainly during overnight hours, with minimal local sources
17 (Borys and Wetzel, 1997). Ambient air was sampled using the Storm Peak facility inlet with
18 the flight PALMS instrument in September, 2015. Measurements were made during Fifth
19 International Ice Nucleation Workshop—phase 3 (FIN03).

20 3 Results

21 Figure 1 shows the spectra of biological species: *P. syringae* bacteria, Snomax and hazelnut
22 pollen wash water particles. These particles contain both organic and inorganic species.
23 Because they are easy to ionize, the inorganic species sodium and potassium stand out in the
24 positive spectra despite their minor fraction by mass. Sulfates, phosphates and nitrates are
25 present, and visible in their associations with potassium. Negative spectra are dominated by
26 CN^- , CNO^- , phosphate (PO_2^- and PO_3^-) and sulfate (HSO_4^-). Higher mass associations of
27 potassium and sulfates, phosphates and nitrates occur ($\text{K}_3\text{H}_2\text{SO}_3^-$, $\text{K}_2\text{H}_3\text{NO}_4^-$, $\text{K}_3\text{H}_2\text{PO}_2^-$ and
28 $\text{K}_3\text{H}_3\text{SO}_3^-$). Chlorine is present on some particles. Chlorine is a known contamination from
29 the Agar growth medium since spectra of aerosolized Agar devoid of bacteria contain large
30 amounts of chlorine (not shown here).



1 Figure 2 shows spectra of apatite. In positive polarity, apatite spectra are dominated by
2 calcium, its oxides, and in associations with phosphate (CaPO^+ , CaPO_2^+ , CaPO_3^+ , Ca_2PO_3^+
3 and Ca_2PO_4^+) and fluorine (CaF^+ , Ca_2OF^+ and Ca_3OF^+). Negative spectra are dominated by
4 phosphates (PO^- , PO_2^- and PO_3^-) and fluorine is often present. Lab-generated apatite spectra
5 analyzed in this study contain little organic. This may be a result of post-processing of the
6 apatite sample, in particular the use of ethanol as a grinding lubricant. In contrast, ethanol was
7 not used in grinding the monazite sample here and its spectra exhibit peaks associated with
8 organic matter (C_2H).

9 Figure 3 shows spectra of coal fly ash from the J. Robert Welsh Power Plant. The positive
10 spectra contain sodium, aluminum, calcium, iron, strontium, barium and lead. As in apatite,
11 calcium/oxygen, calcium/phosphate and calcium/fluorine fragments are present. Fly ash
12 particles also contain sulfate (H_3SO_3^+). The negative spectra contain phosphates (PO_2^- , PO_3^-),
13 sulfates (HSO_4^-) and silicate fragments, such as $(\text{SiO}_2)_2^-$, $(\text{SiO}_2)_2\text{O}^-$, $(\text{SiO}_2)_2\text{Si}^-$ and $(\text{SiO}_2)_3^-$.

14 The results of HNO_3 processing experiments are also shown in Figures 2 and 3. Processing
15 with nitric acid had an effect on both apatite and fly ash: the calcium/fluorine positive
16 markers (CaF^+ , Ca_2OF^+ and Ca_3OF^+) and the negative fluorine marker (F^-) are either reduced
17 in intensity or completely absent after processing. Additionally, CN^- and CNO^- appear and/or
18 intensify after processing.

19 A classifier was designed to use the ratios of phosphate (PO_2^- , PO_3^-) and organic nitrogen
20 (CN^- , CNO^-) spectral peaks. This approach has previously been used with PALMS data to
21 differentiate mineral dusts using silicate and metal peaks to reveal underlying differences in
22 chemistry (Gallavardin et al., 2008). Figure 4A shows normalized histograms of the $\text{PO}_3^-/\text{PO}_2^-$
23 ratio for the test aerosol. The aerosols that contain inorganic phosphorus, such as apatite,
24 monazite, fly ash and soil dust, cluster at $\text{PO}_3^-/\text{PO}_2^- < 4$. The bioaerosols cluster at $\text{PO}_3^-/\text{PO}_2^-$
25 > 2 . Processing of apatite with nitric acid tends to shift the $\text{PO}_3^-/\text{PO}_2^-$ ratio to larger values,
26 increasing the disparity from the bioaerosols. Ragweed pollen is an exception, with a wide
27 cluster in $\text{PO}_3^-/\text{PO}_2^-$ from 1 to 5.

28 A simple delineation can be made based only on the ratio of phosphate peaks at $\text{PO}_3^-/\text{PO}_2^- =$
29 3. The misclassification rate of this simple filter is 20 - 30% for the materials considered here,
30 with ragweed pollen and fly ash as the greatest sources of confusion between the bioaerosol
31 and non-biological classes. A lower misclassification between the bioaerosol and non-
32 biological classes can be achieved if the ratio of organic nitrogen peaks is also taken into



1 account. Figure 4B shows normalized histograms of CN^-/CNO^- ratios for the test aerosol. In
2 contrast to $\text{PO}_3^-/\text{PO}_2^-$ ratios, CN^-/CNO^- ratios do not, by themselves, exhibit a clear difference
3 between the classes. A superior separation is achieved when data are plotted in a CN^-/CNO^-
4 vs. $\text{PO}_3^-/\text{PO}_2^-$ space, as shown in Figure 5. In this case two clusters appear. The soil dust class
5 was left out from the training set because it is not known *a priori* if and how much biological
6 material it contains (classification with the SVM algorithm is discussed latter). The boundary
7 between the classes in CN^-/CNO^- vs. $\text{PO}_3^-/\text{PO}_2^-$ space is non-linear: the SVM algorithm
8 “draws” this boundary, as shown in Figure 5. The misidentification rate in this 2D
9 classification is $\sim 3\%$. As before, ragweed pollen is the cause of most errors; if it is removed
10 from training dataset, the misidentification rate falls to $<1\%$.

11 Once trained with the laboratory data, the SVM algorithm was used to analyze the FIN03
12 field dataset collected at Storm Peak. As a first step, “phosphorus-containing” particles were
13 identified in the dataset. The criterion for phosphorus-containing used for this work is the
14 presence of both PO_2^- and PO_3^- ions at fractional peak area (area of peak of interest/total
15 spectral signal area) greater than 0.01. This threshold was set by examination of the ambient
16 mass spectra to determine when the phosphate peaks are above the noise threshold. Ambient
17 particles commonly have small peaks at masses below ~ 200 due to a diversity of organic
18 components. The height of this background is ~ 0.01 and data below this level are considered
19 uncertain. Phosphorus-containing ambient spectra were then classified by the SVM algorithm
20 as bioaerosol or inorganic phosphorous if the CNO^- ion was also present at fractional peak
21 area greater than 0.001. If CNO^- fractional area was less than 0.001, the spectrum was also
22 classified as inorganic phosphorus.

23 During the FIN03 campaign, phosphorus-containing particles represented from 0.2 to 0.5% by
24 number of the total detected in negative ion mode depending on the sampling day and a 0.4%
25 average for the entire dataset. As shown in Figure 6A when the binary classifier described in
26 this work was applied to the phosphorus-containing particles, bioaerosol represented a 29%
27 subset by number (i.e., 0.1% of total analyzed particles). This is within, and towards the lower
28 end, of previous estimates with biological-specific techniques (Table 1). This lower end
29 estimate may, in part, be due to PALMS sampling particles in the 200-500 nm diameter range
30 as well as larger sizes. Previous estimates tend to show increased bioaerosol in the super-
31 micrometer range and data are often unavailable for the numerous particles smaller than 500
32 nm diameter.



1 The origin of the non-biological phosphate particles is likely phosphate-bearing mineral dust
2 or fly ash. At Storm Peak a likely source is mining of phosphate rock and nearby monazite
3 deposits. Figure 6B shows HYSPLIT back trajectories for the ten days of the FIN03
4 campaign; the air masses sampled cross deposits of either phosphate rock (apatite) or rare
5 earth elements (monazite or carbonatite). As examples, on 09/27 the back trajectory
6 intersects the vicinity of an active REE mine in Mountain Pass, CA and on 09/18 and 09/20
7 the air mass intersected active phosphate mines in Idaho. Although negative spectra of apatite
8 and monazite cannot be definitively differentiated from fly ash or soil dust spectra, positive
9 spectra acquired during FIN03 provide additional evidence that monazite-type material was
10 present. In Figure 2, panels G and H show non-biological phosphate-rich ambient spectra
11 from FIN03. Figure 2 panels E and F (monazite) contains similar features and matching rare
12 earth elements.

13 In total, 56% of phosphate-containing particles analyzed in FIN03 categorized as biological
14 also contained silicate features. Considered in more detail in the next section, a subset of these
15 may represent internal mixtures of biological and mineral components.

16 **4 Discussion**

17 **4.1 Uncertainty in bioaerosol identification in PALMS spectra**

18 The method of identification of bioaerosol described here is based on ratios of phosphate and
19 organic nitrogen peaks. This work is specific to PALMS but can be considered a starting point
20 from which identification and differentiation can be made with similar instruments. Previous
21 work with PALMS shows this ratio approach can be used to identify differences in chemistry,
22 for example among mineral dusts (Gallavardin et al., 2008). In this case the classes are
23 bioaerosol and non-biological phosphorous; Figure 4A shows that phosphorus ionizes
24 differently in these classes. In apatite and monazite, phosphorus occurs as calcium phosphate.
25 In biological particles, phosphorus occurs mostly in phospholipid bilayers and nucleic acids.
26 In these experiments, the $\text{PO}_3^-/\text{PO}_2^-$ ratio of those two forms is different (Figure 4A). The
27 agricultural soils considered here cluster with the minerals and fly ash and we assume the
28 phosphorous is due to the use of inorganic fertilizer, which is derived from calcium phosphate
29 (Koppelaar and Weikard, 2013). Fly ash aerosol clusters similarly to apatite and monazite but
30 with a wider distribution; this is likely because the chemical form of phosphorus in fly ash is
31 different than in the minerals. Phosphorus present in coal is volatilized and then condenses
32 into different forms during the combustion process (Wang et al., 2014).



1 Phosphorus peak ratios in biological particles cluster differently than in inorganic
2 phosphorous particles with ragweed pollen an exception (Figure 4A). No satisfactory
3 explanation for this observation has been found although contamination with phosphate
4 fertilizer cannot be ruled out. The classification error of the biological filter using $\text{PO}_3^-/\text{PO}_2^-$
5 and CN^-/CNO^- ratios is 3% with ragweed alone the source of most of the error. This
6 unexplained behavior is a cause for concern, as the list of biological samples used as a
7 training set is extensive, but not exhaustive and other exceptions could exist.

8 During the FIN03 campaign at Storm Peak, 0.2-0.5% of particles by number detected in
9 negative polarity contained measureable phosphorus (Figure 6A). On most days, the majority
10 of phosphorus-rich particles were inorganic. Particles with positive spectra showing the
11 characteristics of monazite coupled to back trajectories over source areas provides evidence of
12 the origin of the inorganic phosphate particles. Although apatite/monazite particles make up a
13 small portion of ambient particles at Storm Peak they are potentially interesting not only due
14 to their possible confusion with biological phosphate but also as a tracer for industrial mining
15 and processing activities. Currently, such activities are taking place in Idaho and until very
16 recently at Mountain Pass, CA (U.S. Geological Survey, 2016a, 2016b). Smaller exploration
17 activities are also taking place at the Bear Lodge, WY and the REE-rich areas in Colorado,
18 Idaho and Montana are of interest (U.S. Geological Survey, 2016a).

19 **4.2 Comparison with existing literature**

20 Previous studies have attempted to identify bioaerosol with SPMS based on the presence of
21 phosphate and organic nitrate components. Creamean et al. (2013) and Pratt et al. (2009b)
22 suggested a “Boolean criterion” where the existence of CN^- , CNO^- and PO_3^- in a particle
23 resulted in its classification as biological. If a silicate components were additionally present,
24 the particle was classified as an internal mixture of mineral dust and biological components
25 (Creamean et al., 2013; 2014).

26 The selectivity of this simple three-component filter (presence or absence of CN^- , CNO^- and
27 PO_3^-) for biological particles was investigated for PALMS using the test aerosol database with
28 results shown in Figure 7. The filter successfully picks biological material. However, it also
29 has a high rate of false positives. For the material that contains inorganic phosphorus (i.e.,
30 samples known to be devoid of biological material) the three-component filter selects 56% of
31 fly ash, 56% of agricultural dust and 32% of apatite and monazite. Soil dust is identified as
32 biological 78% of the time.



1 The effect of misidentification of inorganic phosphate as biological can be considered in the
2 context of the atmospheric abundance of the three major phosphate bearing aerosols: mineral
3 dust, fly ash and bioaerosol (estimates given in Table 3). Because the emissions estimates
4 vary, the highest fraction of bioaerosol is the case of the highest estimate of bioaerosol
5 coupled to the lowest estimate of fly ash and mineral dust (Table 3 and Figure 8A).
6 Conversely, the lowest fraction of bioaerosol is the case of the lowest estimate of bioaerosol
7 coupled to the highest estimate of fly ash and mineral dust (Table 3 and Figure 8B).

8 The misidentification rates shown above are then propagated onto the high and low estimates.
9 As an example, the fraction of aerosol phosphate due to fly ash (1% in the high and 5% in the
10 low bioaerosol estimate) is multiplied by .56 to indicate the fraction of fly ash that would be
11 misidentified as biological phosphate with the simple three-component filter. This
12 misidentification effect is repeated for the mineral dust emission rate and misidentification
13 fraction. For simplicity, we considered the mineral dust fraction to be desert soils, termed
14 aridsols and entisols, which are predominantly present in dust-productive regions, such as the
15 Sahara or the dust bowl (Yang et al., 2013). According to Yang and Post (2011), the organic
16 phosphate content of those soils is 5-15% but this is a second order effect when compared to
17 misclassification. In the high bioaerosol scenario 17% of the phosphate aerosol is biological
18 (Figure 8A) but when misidentification is considered 81% of particles are identified as such
19 (Figure 8C). In the low bioaerosol scenario 2% of the phosphate aerosol is biological (Figure
20 8B) but when misidentification is considered 77% of the particles are identified as such
21 (Figure 8D). This illustrates that simplistic identification can lead to large misclassification
22 errors of aerosol sources.

23 Misidentification can also lead to misattribution. Pratt et al. (2009b) analyzed ice residuals
24 sampled in an orographic cloud and suggested a biological source using the simple three-
25 component filter applied to spectra containing calcium, sodium, organic carbon, organic
26 nitrogen and phosphate. The processed apatite spectrum in Figure 2, devoid of biological
27 material, contains all of these markers. Similar to the Storm Peak dataset, the Pratt et al.
28 (2009b) wave cloud occurred in west-central Wyoming which is near the Idaho phosphate
29 rock deposits (Figure 6) and four U.S. states with active mining of phosphate rock for use as
30 inorganic fertilizer in agriculture (U.S. Geological Survey, 2016b).

31 The Pratt et al. (2009b) and Creamean et al. (2013, 2014) studies were performed with a
32 different SPMS, the ATOFMS (Gard et al., 1997; Pratt et al., 2009a). Because the ATOFMS



1 uses a desorption/ionization laser of a different wavelength (266 nm) the SVM algorithm used
2 here may not directly translate to that instrument. Instead, the calculation above assumes only
3 that the misidentification rates between the simple three-component filter and the SVM
4 algorithm applies.

5 **4.3 Soil dust and internal dust/biological mixtures**

6 Soil dust is an important but complicated category of phosphate-containing atmospheric
7 particles. Modeling studies, such as Mahowald et al. (2008), treat all phosphorus in soil dust
8 aerosol as inorganic. However, the phosphorus in soil investigated here took both organic and
9 inorganic forms. Walker and Syers (1976) proposed a conceptual model of transformations of
10 phosphorus depending on the age of the soil. At the beginning of its development, all soil
11 phosphorus is bound in its primary mineral form, matching that of the parent material, which
12 is primarily apatite (Walker and Syers, 1976; Yang and Post, 2011). As the soil ages, the
13 primary phosphorus is released. Some of it enters the organic reservoir and is utilized by
14 vegetation, some is adsorbed onto the surface of secondary soil minerals (non-occluded
15 phosphorus) and then gradually encapsulated by secondary minerals (Fe and Al oxides) into
16 an occluded form. The total phosphorus content of the soil decreases as the soil ages, due to
17 leaching. The organic fraction can encompass microorganisms, their metabolic by-products
18 and other biological matter at various stages of decomposition. Soil microorganisms are the
19 key players in converting organic phosphorus back into the mineral form (Brookes et al.,
20 1984). Yang and Post (2011) estimated organic and inorganic phosphorus content of various
21 soils based on available data. Spodosols (moist forest soils) have the highest fraction of
22 organic phosphorus (~45%) and aridsols (sandy desert soils) have the lowest (~5%) (Yang
23 and Post, 2011). Yang et al. (2013) compiled a global map of soil phosphorus distribution and
24 its forms and found that 20%, on average, of total phosphorus is organic. Wang et al. (2010)
25 arrive at 34% of soil phosphorus as organic globally.

26 The biological PALMS filter was applied to several soil dust samples (Table 2) and the
27 numbers of biological particles in all cases fall within these estimates. As would be expected,
28 soils collected in areas with less vegetation exhibit smaller biological contributions. We note
29 that organic phosphorus content is not necessarily a direct indicator of microbes since it also
30 encompasses decomposed organic matter. At this time, we are not able to delineate between
31 primary biological and biogenic or simply complex organic (such as humic acids) material.



1 In the FIN03 field dataset, 56% of particles identified as biological also contained silicate
2 markers normally associated with mineral dust. This represents an upper limit of particles
3 that are an internal mixture of dust and biological material. As stated in the last paragraph,
4 this biological material probably does not consist of whole cells sitting on mineral particles;
5 such internally mixed mineral dust particles with surface whole or fragments of biological
6 material are not supported by EM (Peter Buseck, personal communication, 2016). It currently
7 remains unclear if such internally mixed particles would be counted as biological with an
8 optical microscope after fluorescent staining.

9 Internal mixtures of biological and mineral components were generated in the laboratory in
10 order to investigate this; an exemplary spectrum of such a particle is shown in Figure 9. The
11 spectrum contains aluminosilicate markers consistent with mineral dust together with
12 phosphate markers that, in this case, come from the biological material. Using the classifier
13 developed in this paper on the laboratory-generated internally mixed particles correctly
14 identifies the phosphate signatures to be biological.

15 **5 Conclusion**

16 This paper examines criteria that can be used with SPMS instruments to identify bioaerosol.
17 We propose a new technique of bioaerosol detection and validate it using a database of
18 phosphorus-bearing spectra. A simple binary classification scheme was optimized using a
19 SVM algorithm, with a classification error of 3%. Using the binary classifier developed in this
20 paper, ambient data collected at Storm Peak during the FIN03 campaign was analyzed.
21 Particles with phosphorus were up to 0.5% by number of all ambient particles in the 200 –
22 3000 nm size range. On average, 29% of these particles were identified as biological.

23 Our work expands on previous SPMS sampling that used a more simple Boolean three marker
24 criterion (CN^- , CNO^- and PO_3^-) to classify particles as primary biological or not (Creamean et
25 al., 2013; 2014). We show that the presence of these markers is necessary but not sufficient.
26 We show a false positive rate of the Boolean filter between 64% and 75% for a realistic
27 atmospheric mixture of soil dust, fly ash and primary biological particles.

28 The trained SVM algorithm was also used to measure the biological content of soil dusts.
29 Different soil dust samples can have different content of biological material with a range from
30 2 – 32% observed here. Consistent with the literature, samples taken from areas with
31 vegetation exhibit a higher biological content.



1 **Acknowledgements**

2 The authors gratefully acknowledge funding from NASA grant # NNX13AO15G, NSF grant
3 # AGS-1461347, NSF grant # AGS-1339264, and DOE grant # DE-SC0014487. M. A. Z.
4 acknowledges the support of NASA Earth and Space Science Fellowship. The authors would
5 like to thank Ottmar Moehler and the KIT AIDA facility staff for hosting the FIN01
6 workshop and Gannet Hallar, Ian McCubbin and DRI Storm Peak Laboratory for hosting the
7 FIN03 workshop. The authors thank the entire FIN01 and FIN03 teams for support and Peter
8 Buseck for useful discussions.

9



1 **References**

- 2 Amato, P., Ménéger, M., Sancelme, M., Laj, P., Mailhot, G. and Delort, A.-M.: Microbial
3 population in cloud water at the Puy de Dôme: Implications for the chemistry of clouds,
4 *Atmos. Environ.*, 39(22), 4143–4153, doi:10.1016/j.atmosenv.2005.04.002, 2005.
- 5 Amato, P., Parazols, M., Sancelme, M., Laj, P., Mailhot, G. and Delort, A.-M.:
6 Microorganisms isolated from the water phase of tropospheric clouds at the Puy de Dôme:
7 major groups and growth abilities at low temperatures, *FEMS Microbiol. Ecol.*, 59(2), 242–
8 254, doi:10.1111/j.1574-6941.2006.00199.x, 2007.
- 9 Artaxo, P., Maenhaut, W., Storms, H. and Van Grieken, R.: Aerosol characteristics and
10 sources for the Amazon Basin during the wet season, *J. Geophys. Res.*, 95(D10), 16971,
11 doi:10.1029/JD095iD10p16971, 1990.
- 12 Bauer, H., Kasper-Giebl, A., Löflund, M., Giebl, H., Hitzenberger, R., Zibuschka, F. and
13 Puxbaum, H.: The contribution of bacteria and fungal spores to the organic carbon content of
14 cloud water, precipitation and aerosols, *Atmos. Res.*, 64(1-4), 109–119, doi:10.1016/S0169-
15 8095(02)00084-4, 2002.
- 16 Bauer, H., Schueller, E., Weinke, G., Berger, A., Hitzenberger, R., Marr, I. L. and Puxbaum,
17 H.: Significant contributions of fungal spores to the organic carbon and to the aerosol mass
18 balance of the urban atmospheric aerosol, *Atmos. Environ.*, 42(22), 5542–5549,
19 doi:10.1016/j.atmosenv.2008.03.019, 2008.
- 20 Ben-Hur, A., Horn, D., Siegelmann, H. T. and Vapnik, V.: Support Vector Clustering, *J.*
21 *Mach. Learn. Res.*, 2, 125–137, 2001.
- 22 Berger, V. I., Singer, D. A. and Orris, G. J.: Carbonatites of the world, explored deposits of
23 Nb and REE; database and grade and tonnage models: U.S. Geological Survey Open-File
24 Report 2009-1139, 17 p. and database., 2009.
- 25 Borys, R. D. and Wetzel, M. A.: Storm Peak Laboratory: A Research, Teaching, and Service
26 Facility for the Atmospheric Sciences, *Bull. Am. Meteorol. Soc.*, 78(10), 2115–2123,
27 doi:10.1175/1520-0477(1997)078<2115:SPLART>2.0.CO;2, 1997.
- 28 Bowers, R. M., Lauber, C. L., Wiedinmyer, C., Hamady, M., Hallar, A. G., Fall, R., Knight,
29 R. and Fierer, N.: Characterization of Airborne Microbial Communities at a High-Elevation
30 Site and Their Potential To Act as Atmospheric Ice Nuclei, *Appl. Environ. Microbiol.*,



- 1 75(15), 5121–5130, doi:10.1128/AEM.00447-09, 2009.
- 2 Bowers, R. M., McLetchie, S., Knight, R. and Fierer, N.: Spatial variability in airborne
3 bacterial communities across land-use types and their relationship to the bacterial
4 communities of potential source environments, *ISME J.*, 5(4), 601–612,
5 doi:10.1038/ismej.2010.167, 2011.
- 6 Bowers, R. M., McCubbin, I. B., Hallar, A. G. and Fierer, N.: Seasonal variability in airborne
7 bacterial communities at a high-elevation site, *Atmos. Environ.*, 50, 41–49,
8 doi:10.1016/j.atmosenv.2012.01.005, 2012.
- 9 Brahney, J., Mahowald, N., Ward, D. S., Ballantyne, A. P. and Neff, J. C.: Is atmospheric
10 phosphorus pollution altering global alpine Lake stoichiometry?, *Global Biogeochem. Cycles*,
11 29(9), 1369–1383, doi:10.1002/2015GB005137, 2015.
- 12 Brookes, P. C., Powelson, D. S. and Jenkinson, D. S.: Phosphorus in the soil microbial
13 biomass, *Soil Biol. Biochem.*, 16(2), 169–175, doi:10.1016/0038-0717(84)90108-1, 1984.
- 14 Burrows, S. M., Hoose, C., Pöschl, U. and Lawrence, M. G.: Ice nuclei in marine air: biogenic
15 particles or dust?, *Atmos. Chem. Phys.*, 13(1), 245–267, doi:10.5194/acp-13-245-2013, 2013.
- 16 Buseck, P. R. and Posfai, M.: Airborne minerals and related aerosol particles: Effects on
17 climate and the environment, *Proc. Natl. Acad. Sci.*, 96(7), 3372–3379,
18 doi:10.1073/pnas.96.7.3372, 1999.
- 19 Cahill, J. F., Darlington, T. K., Fitzgerald, C., Schoepp, N. G., Beld, J., Burkart, M. D. and
20 Prather, K. A.: Online Analysis of Single Cyanobacteria and Algae Cells under Nitrogen-
21 Limited Conditions Using Aerosol Time-of-Flight Mass Spectrometry, *Anal. Chem.*, 87(16),
22 8039–8046, doi:10.1021/acs.analchem.5b02326, 2015.
- 23 Chernoff, C. B. and Orris, G. J.: Data set of world phosphate mines, deposits, and
24 occurrences--Part A. Geologic Data; Part B. Location and Mineral Economic Data: U.S.
25 Geological Survey Open-File Report 02-156., 2002.
- 26 Christner, B. C., Cai, R., Morris, C. E., McCarter, K. S., Foreman, C. M., Skidmore, M. L.,
27 Montross, S. N. and Sands, D. C.: Geographic, seasonal, and precipitation chemistry influence
28 on the abundance and activity of biological ice nucleators in rain and snow, *Proc. Natl. Acad.*
29 *Sci.*, 105(48), 18854–18859, doi:10.1073/pnas.0809816105, 2008a.
- 30 Christner, B. C., Morris, C. E., Foreman, C. M., Cai, R. and Sands, D. C.: Ubiquity of



- 1 Biological Ice Nucleators in Snowfall, *Science*, 319(5867), 1214–1214,
2 doi:10.1126/science.1149757, 2008b.
- 3 Cortes, C. and Vapnik, V.: Support-vector networks, *Mach. Learn.*, 20(3), 273–297,
4 doi:10.1007/BF00994018, 1995.
- 5 Creamean, J. M., Suski, K. J., Rosenfeld, D., Cazorla, A., DeMott, P. J., Sullivan, R. C.,
6 White, A. B., Ralph, F. M., Minnis, P., Comstock, J. M., Tomlinson, J. M. and Prather, K. A.:
7 Dust and Biological Aerosols from the Sahara and Asia Influence Precipitation in the Western
8 U.S., *Science*, 339(6127), 1572–1578, doi:10.1126/science.1227279, 2013.
- 9 Creamean, J. M., Lee, C., Hill, T. C., Ault, A. P., DeMott, P. J., White, A. B., Ralph, F. M.
10 and Prather, K. A.: Chemical properties of insoluble precipitation residue particles, *J. Aerosol*
11 *Sci.*, 76, 13–27, doi:10.1016/j.jaerosci.2014.05.005, 2014.
- 12 Cziczo, D. J. and Froyd, K. D.: Sampling the composition of cirrus ice residuals, *Atmos. Res.*,
13 142, 15–31, doi:10.1016/j.atmosres.2013.06.012, 2014.
- 14 Cziczo, D. J., Thomson, D. S. and Murphy, D. M.: Ablation, Flux, and Atmospheric
15 Implications of Meteors Inferred from Stratospheric Aerosol, *Science*, 291(5509), 1772–1775,
16 doi:10.1126/science.1057737, 2001.
- 17 Cziczo, D. J., Thomson, D. S., Thompson, T. L., DeMott, P. J. and Murphy, D. M.: Particle
18 analysis by laser mass spectrometry (PALMS) studies of ice nuclei and other low number
19 density particles, *Int. J. Mass Spectrom.*, 258(1-3), 21–29, doi:10.1016/j.ijms.2006.05.013,
20 2006.
- 21 Cziczo, D. J., Froyd, K. D., Hoose, C., Jensen, E. J., Diao, M., Zondlo, M. A., Smith, J. B.,
22 Twohy, C. H. and Murphy, D. M.: Clarifying the Dominant Sources and Mechanisms of
23 Cirrus Cloud Formation, *Science*, 340, 1320–1324, 2013.
- 24 DeLeon-Rodriguez, N., Latham, T. L., Rodriguez-R, L. M., Barazesh, J. M., Anderson, B. E.,
25 Beyersdorf, A. J., Ziemba, L. D., Bergin, M., Nenes, A. and Konstantinidis, K. T.:
26 Microbiome of the upper troposphere: Species composition and prevalence, effects of tropical
27 storms, and atmospheric implications, *Proc. Natl. Acad. Sci.*, 110(7), 2575–2580,
28 doi:10.1073/pnas.1212089110, 2013.
- 29 DeMott, P. J., Cziczo, D. J., Prenni, A. J., Murphy, D. M., Kreidenweis, S. M., Thomson, D.
30 S., Borys, R. and Rogers, D. C.: Measurements of the concentration and composition of



- 1 nuclei for cirrus formation, *Proc. Natl. Acad. Sci.*, 100(25), 14655–14660,
2 doi:10.1073/pnas.2532677100, 2003.
- 3 Ebert, M., Worrigen, A., Benker, N., Mertes, S., Weingartner, E. and Weinbruch, S.:
4 Chemical composition and mixing-state of ice residuals sampled within mixed phase clouds,
5 *Atmos. Chem. Phys.*, 11(6), 2805–2816, doi:10.5194/acp-11-2805-2011, 2011.
- 6 Fahlgren, C., Hagstrom, A., Nilsson, D. and Zweifel, U. L.: Annual Variations in the
7 Diversity, Viability, and Origin of Airborne Bacteria, *Appl. Environ. Microbiol.*, 76(9), 3015–
8 3025, doi:10.1128/AEM.02092-09, 2010.
- 9 Fang, Z., Ouyang, Z., Zheng, H., Wang, X. and Hu, L.: Culturable Airborne Bacteria in
10 Outdoor Environments in Beijing, China, *Microb. Ecol.*, 54(3), 487–496,
11 doi:10.1007/s00248-007-9216-3, 2007.
- 12 Fergenson, D. P., Pitesky, M. E., Tobias, H. J., Steele, P. T., Czerwieniec, G. A., Russell, S.
13 C., Lebrilla, C. B., Horn, J. M., Coffee, K. R., Srivastava, A., Pillai, S. P., Shih, M.-T. P.,
14 Hall, H. L., Ramponi, A. J., Chang, J. T., Langlois, R. G., Estacio, P. L., Hadley, R. T., Frank,
15 M. and Gard, E. E.: Reagentless Detection and Classification of Individual Bioaerosol
16 Particles in Seconds, *Anal. Chem.*, 76(2), 373–378, doi:10.1021/ac034467e, 2004.
- 17 Friedman, B., Zelenyuk, A., Beranek, J., Kulkarni, G., Pekour, M., Gannet Hallar, A.,
18 McCubbin, I. B., Thornton, J. A. and Cziczo, D. J.: Aerosol measurements at a high-elevation
19 site: composition, size, and cloud condensation nuclei activity, *Atmos. Chem. Phys.*, 13(23),
20 11839–11851, doi:10.5194/acp-13-11839-2013, 2013.
- 21 Froyd, K. D., Murphy, D. M., Lawson, P., Baumgardner, D. and Herman, R. L.: Aerosols that
22 form subvisible cirrus at the tropical tropopause, *Atmos. Chem. Phys.*, 10(1), 209–218,
23 doi:10.5194/acp-10-209-2010, 2010.
- 24 Gabey, A. M., Gallagher, M. W., Whitehead, J., Dorsey, J. R., Kaye, P. H. and Stanley, W.
25 R.: Measurements and comparison of primary biological aerosol above and below a tropical
26 forest canopy using a dual channel fluorescence spectrometer, *Atmos. Chem. Phys.*, 10(10),
27 4453–4466, doi:10.5194/acp-10-4453-2010, 2010.
- 28 Gallavardin, S., Lohmann, U. and Cziczo, D.: Analysis and differentiation of mineral dust by
29 single particle laser mass spectrometry, *Int. J. Mass Spectrom.*, 274(1–3), 56–63,
30 doi:http://dx.doi.org/10.1016/j.ijms.2008.04.031, 2008.



- 1 Gard, E., Mayer, J. E., Morrical, B. D., Dienes, T., Fergenson, D. P. and Prather, K. A.: Real-
2 Time Analysis of Individual Atmospheric Aerosol Particles: Design and Performance of a
3 Portable ATOFMS, *Anal. Chem.*, 69(20), 4083–4091, doi:10.1021/ac970540n, 1997.
- 4 Garimella, S., Huang, Y.-W., Seewald, J. S. and Cziczo, D. J.: Cloud condensation nucleus
5 activity comparison of dry- and wet-generated mineral dust aerosol: the significance of
6 soluble material, *Atmos. Chem. Phys.*, 14(12), 6003–6019, doi:10.5194/acp-14-6003-2014,
7 2014.
- 8 Georgakopoulos, D. G., Després, V., Fröhlich-Nowoisky, J., Psenner, R., Ariya, P. A., Pósfai,
9 M., Ahern, H. E., Moffett, B. F. and Hill, T. C. J.: Microbiology and atmospheric processes:
10 biological, physical and chemical characterization of aerosol particles, *Biogeosciences*, 6(4),
11 721–737, doi:10.5194/bg-6-721-2009, 2009.
- 12 Griffin, D. W., Garrison, V. H., Herman, J. R. and Shinn, E. A.: African desert dust in the
13 Caribbean atmosphere: Microbiology and public health, *Aerobiologia (Bologna)*, 17(3), 203–
14 213, doi:10.1023/A:1011868218901, 2001.
- 15 Griffin, D. W., Westphal, D. L. and Gray, M. A.: Airborne microorganisms in the African
16 desert dust corridor over the mid-Atlantic ridge, *Ocean Drilling Program, Leg 209*,
17 *Aerobiologia (Bologna)*, 22(3), 211–226, doi:10.1007/s10453-006-9033-z, 2006.
- 18 Harrison, R. M., Jones, A. M., Biggins, P. D. E., Pomeroy, N., Cox, C. S., Kidd, S. P.,
19 Hobman, J. L., Brown, N. L. and Beswick, A.: Climate factors influencing bacterial count in
20 background air samples, *Int. J. Biometeorol.*, 49(3), 167–178, doi:10.1007/s00484-004-0225-
21 3, 2005.
- 22 Hill, S. C., Pinnick, R. G., Niles, S., Pan, Y.-L., Holler, S., Chang, R. K., Bottiger, J., Chen,
23 B. T., Orr, C.-S. and Feather, G.: Real-time measurement of fluorescence spectra from single
24 airborne biological particles, *F. Anal. Chem. Technol.*, 3(4-5), 221–239,
25 doi:10.1002/(SICI)1520-6521(1999)3:4/5<221::AID-FACT2>3.0.CO;2-7, 1999.
- 26 Hiranuma, N., Möhler, O., Yamashita, K., Tajiri, T., Saito, A., Kiselev, A., Hoffmann, N.,
27 Hoose, C., Jantsch, E., Koop, T. and Murakami, M.: Ice nucleation by cellulose and its
28 potential contribution to ice formation in clouds, *Nat. Geosci.*, 8(4), 273–277,
29 doi:10.1038/ngeo2374, 2015.
- 30 Hoose, C., Kristjánsson, J. E. and Burrows, S. M.: How important is biological ice nucleation
31 in clouds on a global scale?, *Environ. Res. Lett.*, 5(2), 024009, doi:10.1088/1748-



- 1 9326/5/2/024009, 2010.
- 2 Jacobson, M. Z. and Streets, D. G.: Influence of future anthropogenic emissions on climate,
3 natural emissions, and air quality, *J. Geophys. Res.*, 114(D8), D08118,
4 doi:10.1029/2008JD011476, 2009.
- 5 Kaye, P. H., Barton, J. E., Hirst, E. and Clark, J. M.: Simultaneous light scattering and
6 intrinsic fluorescence measurement for the classification of airborne particles, *Appl. Opt.*,
7 39(21), 3738, doi:10.1364/AO.39.003738, 2000.
- 8 Kaye, P. H., Stanley, W. R., Hirst, E., Foot, E. V., Baxter, K. L. and Barrington, S. J.: Single
9 particle multichannel bio-aerosol fluorescence sensor, *Opt. Express*, 13(10), 3583,
10 doi:10.1364/OPEX.13.003583, 2005.
- 11 Koppelaar, R. H. E. M. and Weikard, H. P.: Assessing phosphate rock depletion and
12 phosphorus recycling options, *Glob. Environ. Chang.*, 23(6), 1454–1466,
13 doi:10.1016/j.gloenvcha.2013.09.002, 2013.
- 14 Li, J., Pósfai, M., Hobbs, P. V. and Buseck, P. R.: Individual aerosol particles from biomass
15 burning in southern Africa: 2, Compositions and aging of inorganic particles, *J. Geophys.*
16 *Res. Atmos.*, 108(D13), n/a–n/a, doi:10.1029/2002JD002310, 2003a.
- 17 Li, J., Anderson, J. R. and Buseck, P. R.: TEM study of aerosol particles from clean and
18 polluted marine boundary layers over the North Atlantic, *J. Geophys. Res.*, 108(D6), 4189,
19 doi:10.1029/2002JD002106, 2003b.
- 20 Mahowald, N., Jickells, T. D., Baker, A. R., Artaxo, P., Benitez-Nelson, C. R., Bergametti,
21 G., Bond, T. C., Chen, Y., Cohen, D. D., Herut, B., Kubilay, N., Losno, R., Luo, C.,
22 Maenhaut, W., McGee, K. A., Okin, G. S., Siefert, R. L. and Tsukuda, S.: Global distribution
23 of atmospheric phosphorus sources, concentrations and deposition rates, and anthropogenic
24 impacts, *Global Biogeochem. Cycles*, 22(4), n/a–n/a, doi:10.1029/2008GB003240, 2008.
- 25 Mahowald, N. M., Artaxo, P., Baker, A. R., Jickells, T. D., Okin, G. S., Randerson, J. T. and
26 Townsend, A. R.: Impacts of biomass burning emissions and land use change on Amazonian
27 atmospheric phosphorus cycling and deposition, *Global Biogeochem. Cycles*, 19(4), n/a–n/a,
28 doi:10.1029/2005GB002541, 2005.
- 29 Matthias-Maser, S. and Jaenicke, R.: Examination of atmospheric bioaerosol particles with
30 radii $\geq 0.2 \mu\text{m}$, *J. Aerosol Sci.*, 25(8), 1605–1613, doi:10.1016/0021-8502(94)90228-3,



- 1 1994.
- 2 Möhler, O., Georgakopoulos, D. G., Morris, C. E., Benz, S., Ebert, V., Hunsmann, S.,
3 Saathoff, H., Schnaiter, M. and Wagner, R.: Heterogeneous ice nucleation activity of bacteria:
4 new laboratory experiments at simulated cloud conditions, *Biogeosciences*, 5(5), 1425–1435,
5 doi:10.5194/bg-5-1425-2008, 2008.
- 6 Murphy, D. M.: The design of single particle laser mass spectrometers, *Mass Spectrom. Rev.*,
7 26(2), 150–165, doi:10.1002/mas.20113, 2007.
- 8 Murphy, D. M., Cziczko, D. J., Hudson, P. K., Thomson, D. S., Wilson, J. C., Kojima, T. and
9 Buseck, P. R.: Particle Generation and Resuspension in Aircraft Inlets when Flying in Clouds,
10 *Aerosol Sci. Technol.*, 38(4), 401–409, doi:10.1080/02786820490443094, 2004.
- 11 O'Connor, D. J., Healy, D. A., Hellebust, S., Buters, J. T. M. and Sodeau, J. R.: Using the
12 WIBS-4 (Waveband Integrated Bioaerosol Sensor) Technique for the On-Line Detection of
13 Pollen Grains, *Aerosol Sci. Technol.*, 48(4), 341–349, doi:10.1080/02786826.2013.872768,
14 2014.
- 15 Orris, G. J. and Grauch, R. I.: Rare earth element mines, deposits, and occurrences: U.S.
16 Geological Survey, Open-File Report 02-189., 2002.
- 17 Pan, Y., Holler, S., Chang, R. K., Hill, S. C., Pinnick, R. G., Niles, S. and Bottiger, J. R.:
18 Single-shot fluorescence spectra of individual micrometer-sized bioaerosols illuminated by a
19 351- or a 266-nm ultraviolet laser, *Opt. Lett.*, 24(2), 116, doi:10.1364/OL.24.000116, 1999.
- 20 Pósfai, M., Anderson, J. R., Buseck, P. R., Shattuck, T. W. and Tindale, N. W.: Constituents
21 of a remote pacific marine aerosol: A tem study, *Atmos. Environ.*, 28(10), 1747–1756,
22 doi:10.1016/1352-2310(94)90137-6, 1994.
- 23 Pósfai, M., Anderson, J. R., Buseck, P. R. and Sievering, H.: Compositional variations of sea-
24 salt-mode aerosol particles from the North Atlantic, *J. Geophys. Res.*, 100(D11), 23063,
25 doi:10.1029/95JD01636, 1995.
- 26 Pósfai, M., Li, J., Anderson, J. R. and Buseck, P. R.: Aerosol bacteria over the Southern
27 Ocean during ACE-1, *Atmos. Res.*, 66(4), 231–240, doi:10.1016/S0169-8095(03)00039-5,
28 2003a.
- 29 Pósfai, M., Simonics, R., Li, J., Hobbs, P. V. and Buseck, P. R.: Individual aerosol particles
30 from biomass burning in southern Africa: 1. Compositions and size distributions of



- 1 carbonaceous particles, *J. Geophys. Res. Atmos.*, 108(D13), n/a–n/a,
2 doi:10.1029/2002JD002291, 2003b.
- 3 Pratt, K. A., Mayer, J. E., Holecek, J. C., Moffet, R. C., Sanchez, R. O., Rebotier, T. P.,
4 Furutani, H., Gonin, M., Fuhrer, K., Su, Y., Guazzotti, S. and Prather, K. A.: Development
5 and Characterization of an Aircraft Aerosol Time-of-Flight Mass Spectrometer, *Anal. Chem.*,
6 81(5), 1792–1800, doi:10.1021/ac801942r, 2009a.
- 7 Pratt, K. A., DeMott, P. J., French, J. R., Wang, Z., Westphal, D. L., Heymsfield, A. J.,
8 Twohy, C. H., Prenni, A. J. and Prather, K. A.: In situ detection of biological particles in
9 cloud ice-crystals, *Nat. Geosci.*, 2, 398–401, 2009b.
- 10 Prenni, A. J., Petters, M. D., Kreidenweis, S. M., Heald, C. L., Martin, S. T., Artaxo, P.,
11 Garland, R. M., Wollny, A. G. and Pöschl, U.: Relative roles of biogenic emissions and
12 Saharan dust as ice nuclei in the Amazon basin, *Nat. Geosci.*, 2(6), 402–405,
13 doi:10.1038/ngeo517, 2009.
- 14 Prospero, J. M., Blades, E., Mathison, G. and Naidu, R.: Interhemispheric transport of viable
15 fungi and bacteria from Africa to the Caribbean with soil dust, *Aerobiologia (Bologna)*,
16 21(1), 1–19, doi:10.1007/s10453-004-5872-7, 2005.
- 17 Pruppacher, H. R. and Klett, J. D.: *Microphysics of Clouds and Precipitation*, 2nd ed., Kluwer
18 Academic Publishers, Norwell, MA., 2003.
- 19 Sattler, B., Puxbaum, H. and Psenner, R.: Bacterial growth in supercooled cloud droplets,
20 *Geophys. Res. Lett.*, 28(2), 239–242, doi:10.1029/2000GL011684, 2001.
- 21 Sesartic, A., Lohmann, U. and Storelvmo, T.: Bacteria in the ECHAM5-HAM global climate
22 model, *Atmos. Chem. Phys.*, 12(18), 8645–8661, doi:10.5194/acp-12-8645-2012, 2012.
- 23 Sesartic, A., Lohmann, U. and Storelvmo, T.: Modelling the impact of fungal spore ice nuclei
24 on clouds and precipitation, *Environ. Res. Lett.*, 8(1), 014029, doi:10.1088/1748-
25 9326/8/1/014029, 2013.
- 26 Smith, D. J. and Griffin, D. W.: Inadequate methods and questionable conclusions in
27 atmospheric life study, *Proc. Natl. Acad. Sci.*, 110(23), E2084–E2084,
28 doi:10.1073/pnas.1302612110, 2013.
- 29 Smith, D. J., Jaffe, D. A., Birmele, M. N., Griffin, D. W., Schuerger, A. C., Hee, J. and
30 Roberts, M. S.: Free Tropospheric Transport of Microorganisms from Asia to North America,



- 1 Microb. Ecol., 64(4), 973–985, doi:10.1007/s00248-012-0088-9, 2012.
- 2 Smith, D. J., Timonen, H. J., Jaffe, D. A., Griffin, D. W., Birmele, M. N., Perry, K. D., Ward,
3 P. D. and Roberts, M. S.: Intercontinental Dispersal of Bacteria and Archaea by Transpacific
4 Winds, Appl. Environ. Microbiol., 79(4), 1134–1139, doi:10.1128/AEM.03029-12, 2013.
- 5 Sodeman, D. A., Toner, S. M. and Prather, K. A.: Determination of Single Particle Mass
6 Spectral Signatures from Light-Duty Vehicle Emissions, Environ. Sci. Technol., 39(12),
7 4569–4580, doi:10.1021/es0489947, 2005.
- 8 Spracklen, D. V. and Heald, C. L.: The contribution of fungal spores and bacteria to regional
9 and global aerosol number and ice nucleation immersion freezing rates, Atmos. Chem. Phys.,
10 14(17), 9051–9059, doi:10.5194/acp-14-9051-2014, 2014.
- 11 Steinke, I., Funk, R., Busse, J., Iturri, A., Kirchen, S., Leue, M., Möhler, O., Schwartz, T.,
12 Schnaiter, M., Sierau, B., Toprak, E., Ullrich, R., Ulrich, A., Hoose, C. and Leisner, T.: Ice
13 nucleation activity of agricultural soil dust aerosols from Mongolia, Argentina, and Germany,
14 J. Geophys. Res. Atmos., doi:10.1002/2016JD025160, 2016.
- 15 Thomson, D. S., Schein, M. E. and Murphy, D. M.: Particle analysis by laser mass
16 spectrometry {WB}-57 instrument overview, Aerosol Sci. Technol., 33, 153–169, 2000.
- 17 Toprak, E. and Schnaiter, M.: Fluorescent biological aerosol particles measured with the
18 Waveband Integrated Bioaerosol Sensor WIBS-4: laboratory tests combined with a one year
19 field study, Atmos. Chem. Phys., 13(1), 225–243, doi:10.5194/acp-13-225-2013, 2013.
- 20 Twohy, C. H., McMeeking, G. R., DeMott, P. J., McCluskey, C. S., Hill, T. C. J., Burrows, S.
21 M., Kulkarni, G. R., Tanarhte, M., Kafle, D. N. and Toohey, D. W.: Abundance of fluorescent
22 biological aerosol particles at temperatures conducive to the formation of mixed-phase and
23 cirrus clouds, Atmos. Chem. Phys., 16(13), 8205–8225, doi:10.5194/acp-16-8205-2016, 2016.
- 24 U.S. Geological Survey: 2013 Minerals Yearbook. Rare Earths., 2016a.
- 25 U.S. Geological Survey: Mineral commodity summaries 2016. [online] Available from:
26 <http://dx.doi.org/10.3133/70140094>, 2016b.
- 27 Walker, T. W. and Syers, J. K.: The fate of phosphorus during pedogenesis, Geoderma, 15(1),
28 1–19, doi:10.1016/0016-7061(76)90066-5, 1976.
- 29 Wang, R., Balkanski, Y., Boucher, O., Ciais, P., Peñuelas, J. and Tao, S.: Significant
30 contribution of combustion-related emissions to the atmospheric phosphorus budget, Nat.



- 1 Geosci., 8(1), 48–54, doi:10.1038/ngeo2324, 2014.
- 2 Wang, Y. P., Law, R. M. and Pak, B.: A global model of carbon, nitrogen and phosphorus
3 cycles for the terrestrial biosphere, *Biogeosciences*, 7(7), 2261–2282, doi:10.5194/bg-7-2261-
4 2010, 2010.
- 5 Wiedinmyer, C., Bowers, R. M., Fierer, N., Horanyi, E., Hannigan, M., Hallar, A. G.,
6 McCubbin, I. and Baustian, K.: The contribution of biological particles to observed
7 particulate organic carbon at a remote high altitude site, *Atmos. Environ.*, 43(28), 4278–4282,
8 doi:10.1016/j.atmosenv.2009.06.012, 2009.
- 9 Xia, X., Wang, J., Ji, J., Zhang, J., Chen, L. and Zhang, R.: Bacterial Communities in Marine
10 Aerosols Revealed by 454 Pyrosequencing of the 16S rRNA Gene*, *J. Atmos. Sci.*, 72(8),
11 2997–3008, doi:10.1175/JAS-D-15-0008.1, 2015.
- 12 Xia, Y., Conen, F. and Alewell, C.: Total bacterial number concentration in free tropospheric
13 air above the Alps, *Aerobiologia (Bologna)*, 29(1), 153–159, doi:10.1007/s10453-012-9259-
14 x, 2013.
- 15 Yang, X. and Post, W. M.: Phosphorus transformations as a function of pedogenesis: A
16 synthesis of soil phosphorus data using Hedley fractionation method, *Biogeosciences*, 8(10),
17 2907–2916, doi:10.5194/bg-8-2907-2011, 2011.
- 18 Yang, X., Post, W. M., Thornton, P. E. and Jain, A.: The distribution of soil phosphorus for
19 global biogeochemical modeling, *Biogeosciences*, 10(4), 2525–2537, doi:10.5194/bg-10-
20 2525-2013, 2013.
- 21 Zender, C. S.: Mineral Dust Entrainment and Deposition (DEAD) model: Description and
22 1990s dust climatology, *J. Geophys. Res.*, 108(D14), 4416, doi:10.1029/2002JD002775,
23 2003.
- 24 Zhang, X., Smith, K. A., Worsnop, D. R., Jimenez, J., Jayne, J. T. and Kolb, C. E.: A
25 Numerical Characterization of Particle Beam Collimation by an Aerodynamic Lens-Nozzle
26 System: Part I. An Individual Lens or Nozzle, *Aerosol Sci. Technol.*, 36(5), 617–631,
27 doi:10.1080/02786820252883856, 2002.
- 28 Zhang, X., Smith, K. A., Worsnop, D. R., Jimenez, J. L., Jayne, J. T., Kolb, C. E., Morris, J.
29 and Davidovits, P.: Numerical Characterization of Particle Beam Collimation: Part II
30 Integrated Aerodynamic-Lens-Nozzle System, *Aerosol Sci. Technol.*, 38(6), 619–638,



- 1 doi:10.1080/02786820490479833, 2004.
- 2 Ziemba, L. D., Beyersdorf, A. J., Chen, G., Corr, C. A., Crumeyrolle, S. N., Diskin, G.,
- 3 Hudgins, C., Martin, R., Mikoviny, T., Moore, R., Shook, M., Thornhill, K. L., Winstead, E.
- 4 L., Wisthaler, A. and Anderson, B. E.: Airborne observations of bioaerosol over the Southeast
- 5 United States using a Wideband Integrated Bioaerosol Sensor, J. Geophys. Res. Atmos.,
- 6 doi:10.1002/2015JD024669, 2016.
- 7



- 1 Table 1. Measurements of biological aerosol in the atmosphere (NR – not reported, FBAP – fluorescent particles, attributed to bioaerosol).
- 2 *Comment in response to DeLeon-Rodriguez et al., 2013 by Smith and Griffin (2013).

Site	Elevation (m)	Technique	Concentration of bioaerosol detected (particles m ⁻³)	% of total particles (size range)	Type of bioaerosol	Reference
Ground sites						
Jungfrauoch	3,450	Fluorescent microscopy	3.4×10 ³ (free troposphere) 7.5×10 ⁴ (over surface)	NR	Bacteria	Xia et al., 2013
Storm Peak Lab	3,220	Fluorescent microscopy	9.6×10 ⁵ – 6.6×10 ⁶	0.5-5% (0.5-20 μm)	Bacteria (51%) Fungi (45%) Plant material (4%)	Wiedinmyer et al., 2009
Storm Peak Lab	3,220	Fluorescent microscopy	3.9×10 ⁵ (spring) 4.0×10 ⁴ (summer) 1.5×10 ⁵ (fall) 2.7×10 ⁴ (winter)	22% (0.5-20 μm)	Bacteria	Bowers et al., 2012
Mt. Rax (Alps)	1,644	Fluorescent microscopy	1.1×10 ⁴ (bacteria) 3.5×10 ² (fungi)	NR	Bacteria and fungi	Bauer et al., 2002
Various locations in Colorado	1,485-2,973	Fluorescent microscopy	1.0×10 ⁵ - 2.6×10 ⁶	NR	Bacteria	Bowers et al., 2011
Vienna	150-550	Fluorescent microscopy	3.6×10 ³ – 2.9×10 ⁴	NR	Fungi	Bauer et al., 2008
U.S. Virgin Islands	NR	Fluorescent microscopy	3.6×10 ⁴ – 5.7×10 ⁵	NR	Bacteria and possible viruses	Griffin et al., 2001
Various sites in the U.K.	50-130	Fluorescent microscopy	5.3×10 ³ – 1.7×10 ⁴ (spring) 8.3×10 ³ – 1.5×10 ⁴ (summer) 6.0×10 ³ – 1.4×10 ⁴ (fall) 2.9×10 ³ – 1.0×10 ⁴ (winter)	NR	Bacteria	Harrison et al., 2005
Danum Valley, Malaysian Borneo	150-1,000	WIBS	2.0×10 ⁵ (above forest canopy)	NR	FBAP	Gabey et al., 2010



Karlsruhe, Germany	112	WIBS	1.5×10^6 (below forest canopy) 2.9×10^4 (spring) 4.6×10^4 (summer) 2.9×10^4 (fall) 1.9×10^4 (winter)	4-11% (0.5-16 μm)	FBAP	Toprak and Schnaiter, 2013
Aircraft campaigns						
Cape Grim	30-5,400	TEM	NR	1% ($>0.2 \mu\text{m}$)	Bacteria	Pósfai et al., 2003
Flights around the Gulf of Mexico, California and Florida	3,000-10,000	Fluorescent microscopy	$3.6 \times 10^4 - 3.0 \times 10^5$	3.6-276% (0.25-1 μm)*	Mostly bacteria	DeLeon-Rodriguez et al., 2013
Flights over southeastern U.S. (SEAC ⁴ RS)	Vertical profiles up to 12,000	WIBS	3.4×10^5 (average, $<0.5 \text{ km}$) 7.0×10^4 (average, 3 km) 1.8×10^4 (average, 6 km)	5-10% (0.6-5 μm)	FBAP	Ziemba et al., 2016
Flights over Colorado, Wyoming, Nebraska and South Dakota	Vertical profiles up to 10,000	WIBS	$1.0 \times 10^4 - 1.0 \times 10^5$ ($<2.5 \text{ km}$) $0 - 3.0 \times 10^3$ ($>2.5 \text{ km}$)	NR	FBAP	Twohy et al., 2016

1



- 1 Table 2. Soil dust samples used in this work. The last column shows the results of analysis
- 2 with the biological filter developed here as a percentage of negative particles sampled.

Sample	Site description	Approx. collection coordinates	% biological
Bächli	Outflow sediment of a glacier in a feldspar-rich granitic environment. No vegetation.	46.6 N, 8.3 E	6.0
Morocco	Rock desert with vegetation. Close proximity to a road.	33.2 N, 2.0 W	20.4
Ethiopia	Collected in Lake Shala National Park from a region between two lakes. Area vegetated by shrubs and acacia trees.	7.5 N, 38.7 E	32.1
Storm Peak Lab	Collected near Storm Peak Lab. Grass and shrubs present.	40.5 N, 106.7 W	31.3
Argentina	La Pampa province. Top soil collected from arable land with sandy loam (Steinke et al., 2016).	37 S, 64 W (approximate)	21.3
China/Inner Mongolia	Xilingele steppe. Top soil collected from a pasture with loam (Steinke et al., 2016).	44 N, 117 E (approximate)	2.0
Saudi Arabia	Various samples from several locations. Arid, sandy soils.	24.6 N – 26.3 N, 46.1 E – 49.6 E	14.5

3

4

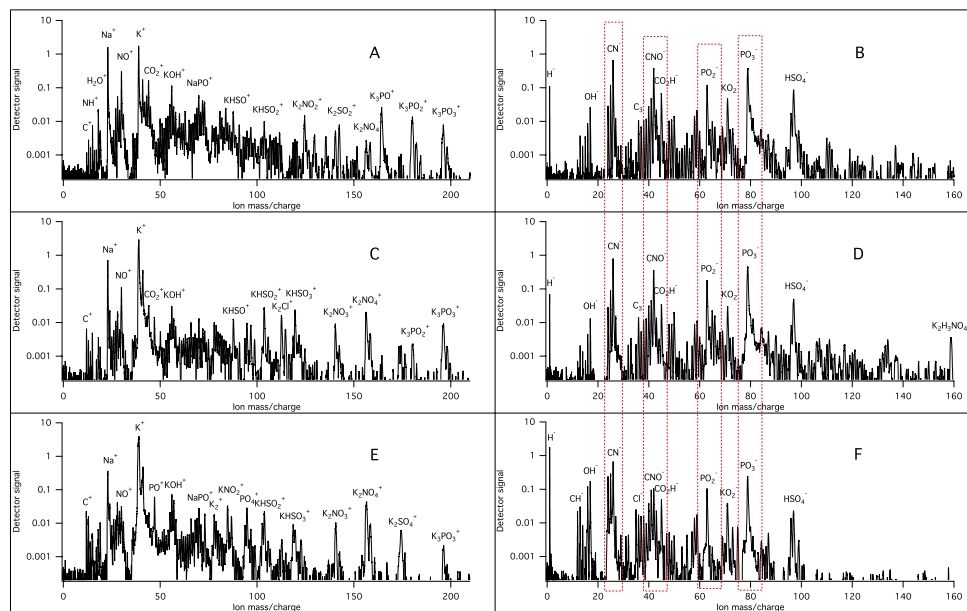


- 1 Table 3. Literature estimates of emission rates of primary biological particles, dust and fly
2 ash.

Particle	Emissions (Tg yr ⁻¹)	
	<i>low estimate</i>	<i>high estimate</i>
Dust	1490 (Zender, 2003)	7800 (Jacobson and Streets, 2009)
Primary biological	186 (Mahowald et al., 2008)	298 (Jacobson and Streets, 2009)
Fly ash	14.9 (Garimella et al., 2016)	390 (Garimella et al., 2016)

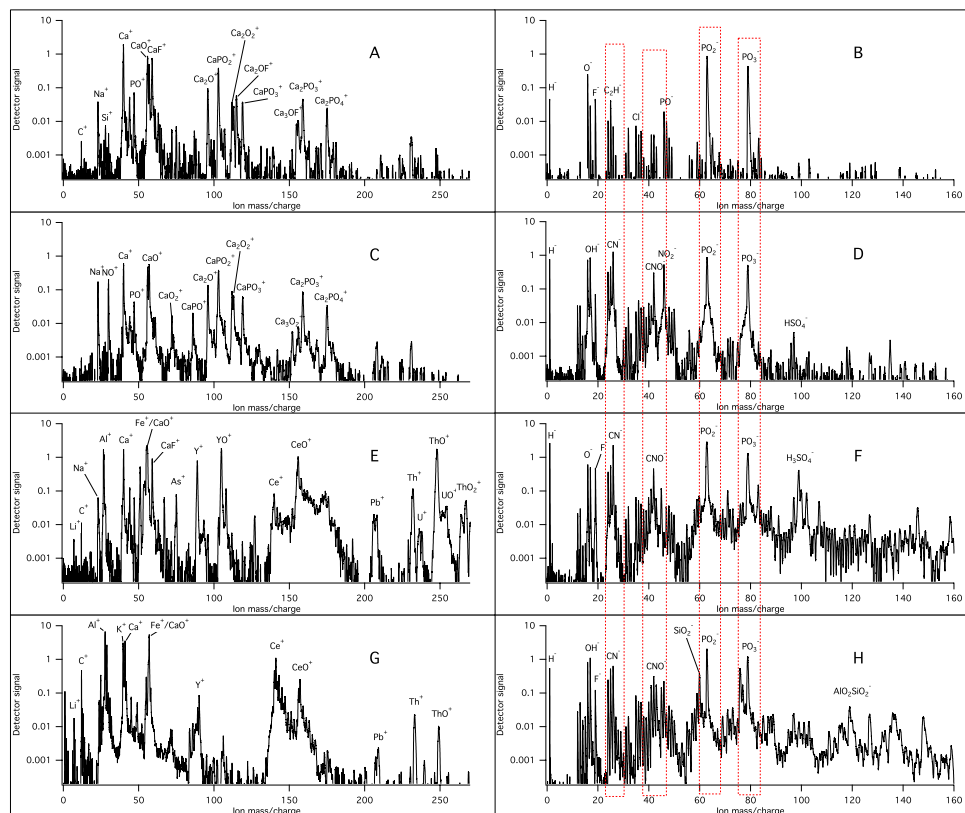
3

4

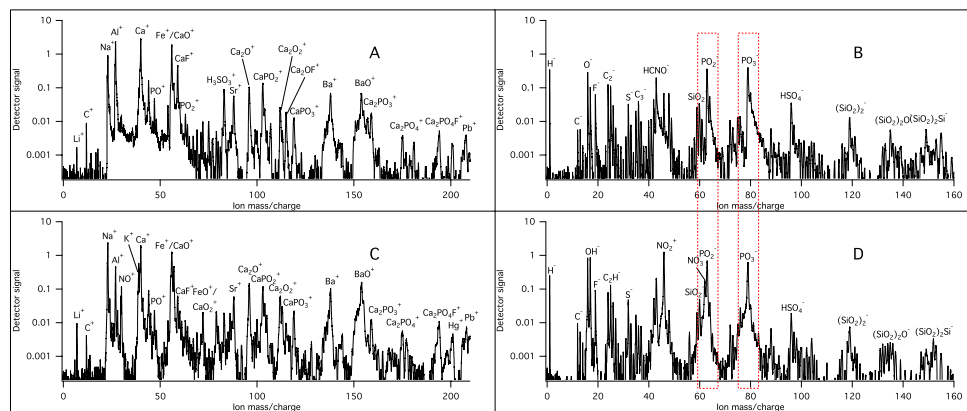


1

2 Figure 1. Representative PALMS spectra of bioaerosol. A and B: Snomax. C and D: *P.*
3 *syringae*. E and F: Hazelnut wash water. Right and left columns are positive and negative
4 polarity, respectively. Red dotted lines are features indicated in the literature as markers for
5 biological material.



1
2 Figure 2. Representative PALMS spectra of phosphorus-rich minerals and ambient aerosol. A
3 and B: Unprocessed apatite. C and D: Apatite processed with HNO₃ (see text for details). E
4 and F: Monazite-Ce. G and H: Ambient particles sampled at Storm Peak matching monazite
5 chemistry. Right and left columns are positive and negative polarity, respectively. Red dotted
6 lines are features indicated in the literature as markers for biological material.
7



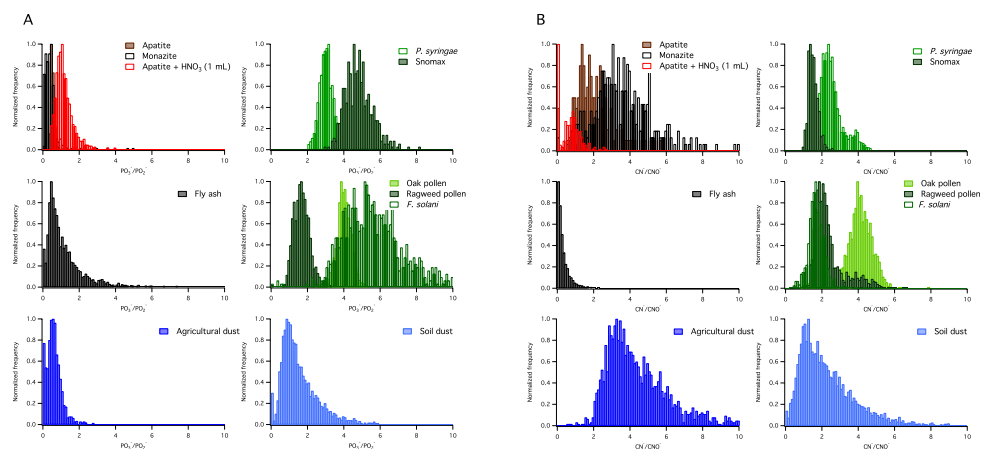
1

2 Figure 3. Representative PALMS spectra of coal fly ash from the J. Robert Welsh power
3 plant. A and B: Unprocessed fly ash. C and D: Fly ash processed with HNO_3 (see text for
4 details). Right and left columns are positive and negative polarity, respectively. Red dotted
5 lines are features indicated in the literature as markers for biological material.

6

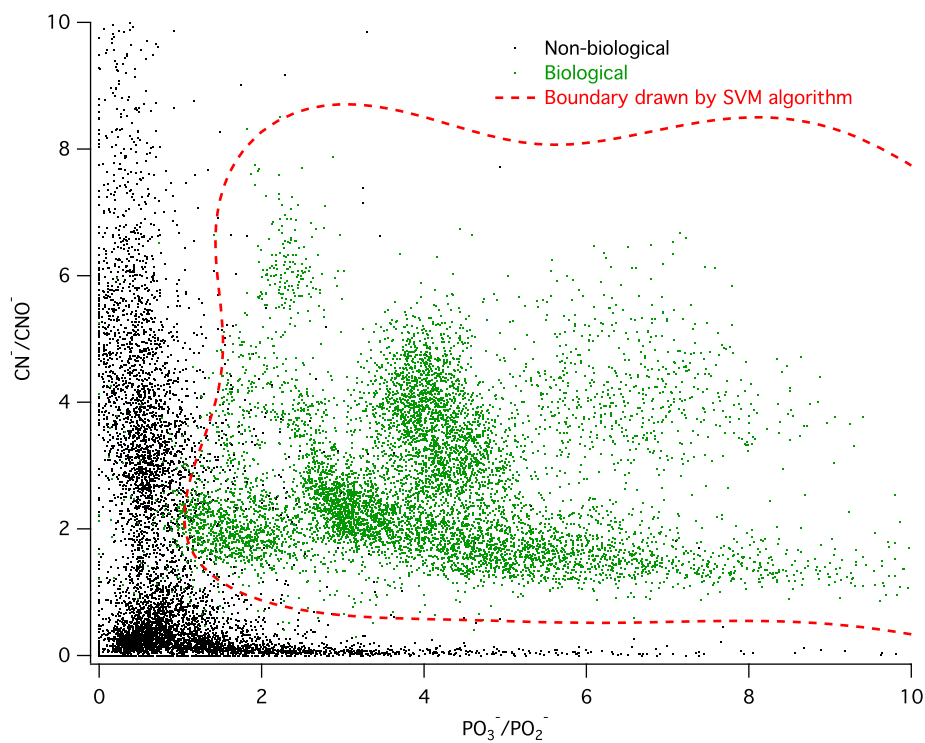


1



2

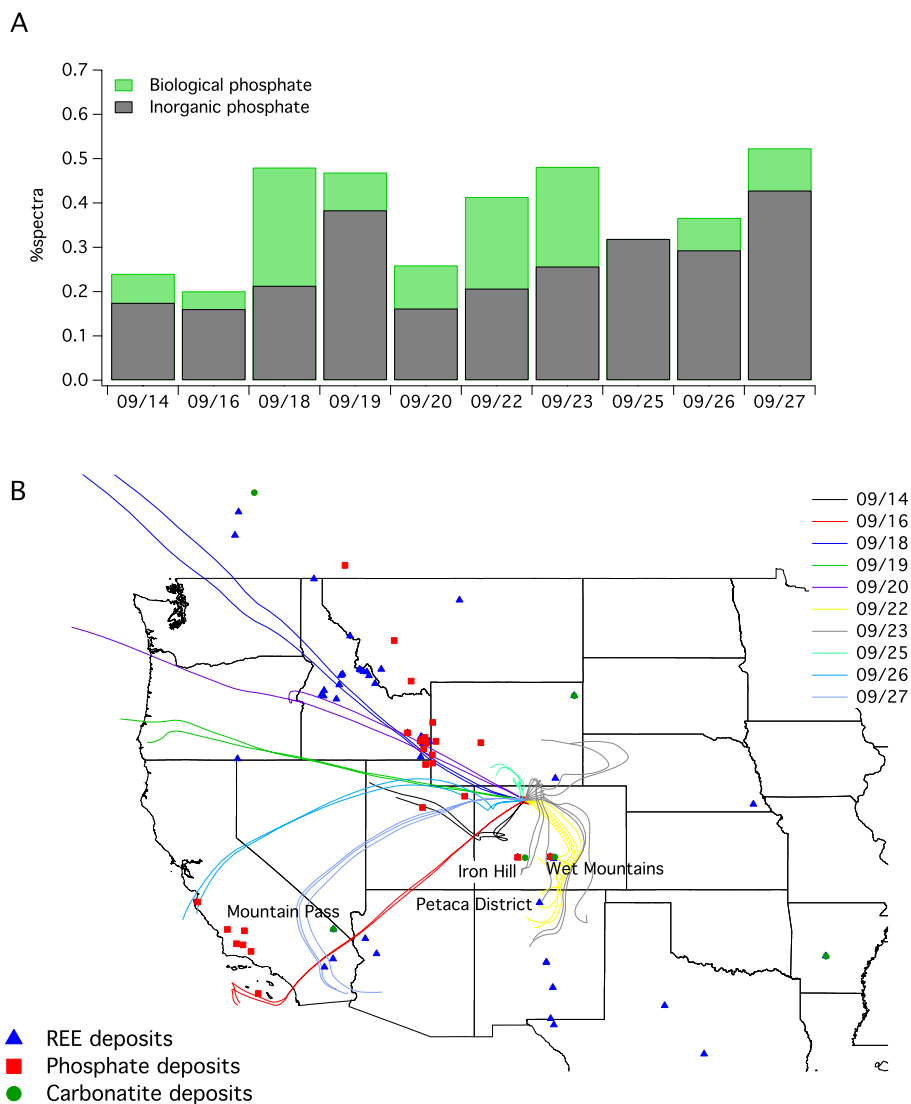
3 Figure 4. A: Normalized histograms of the $\text{PO}_3^-/\text{PO}_2^-$ ratio for the test aerosol. B: Normalized
4 histograms of the CN^-/CNO^- ratio for the same test aerosol as in A. Delineation between the
5 clusters at a $\text{PO}_3^-/\text{PO}_2^-$ ratio of 3 results in a 70-80% classification accuracy depending on the
6 species considered.



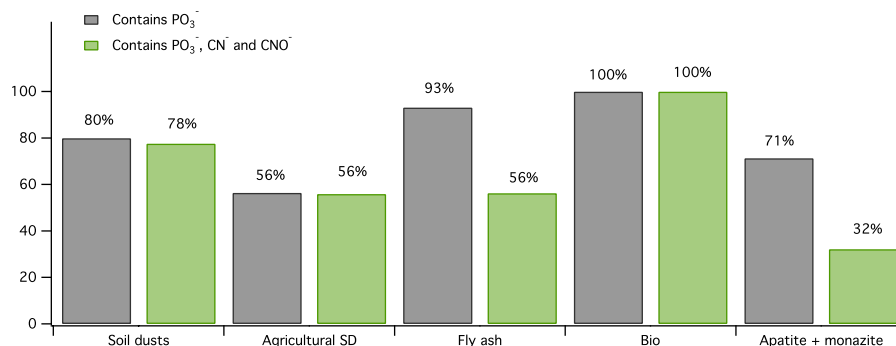
1

2 Figure 5. Inorganic and biological particle clusters in CN^-/CNO^- vs. $\text{PO}_3^-/\text{PO}_2^-$ space. The
3 SVM algorithm delineates between the clusters with the red dashed line with an overall 97%
4 classification accuracy.

5

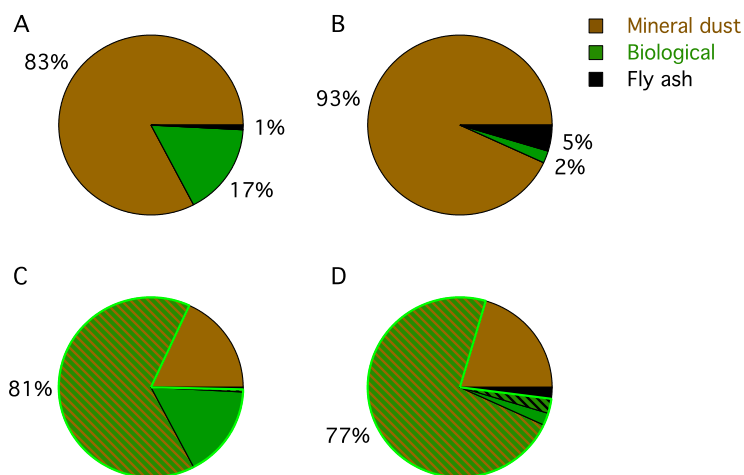


1
2 Figure 6. A: The percentage of ambient aerosol particles from the dataset categorized as
3 biological and inorganic (phosphate-bearing mineral dust or fly ash) phosphate using the
4 criteria developed in this work. Note that at this location and time of year inorganic phosphate
5 dominates biological. B: HYSPLIT back trajectories plotted for ten measurement days at
6 Storm Peak Laboratory. Locations of REE, phosphate and carbonatite deposits, sourced from
7 U.S. Geological Survey, are co-plotted (Berger et al., 2009; Chernoff and Orris, 2002; Orris
8 and Grauch, 2002).

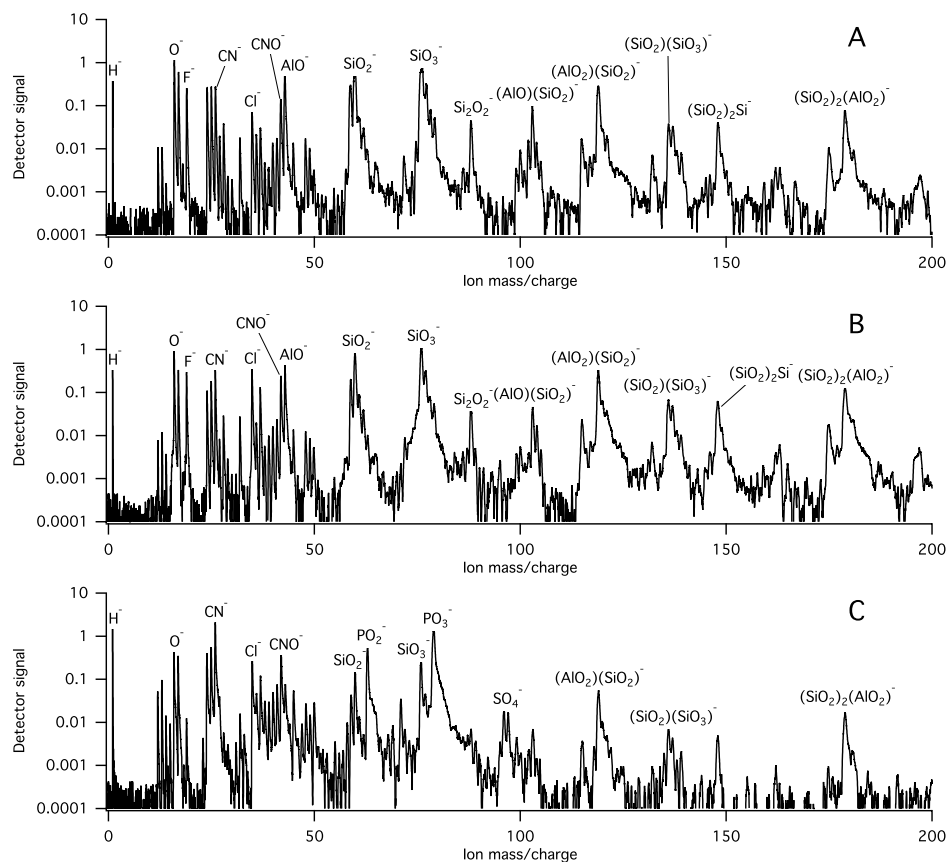


1

2 Figure 7. Percentage of particles that include PO₃⁻, CN⁻ and CNO⁻ markers in five classes of
3 atmospherically-relevant aerosol spectra acquired with PALMS in this work. Note that the
4 green bars indicate the percentage of particles of each type identified as biological using
5 literature criteria. In the case of bioaerosol the identification is correct. In all other aerosol
6 classes the green bar denotes a level of misidentification.



1
2 Figure 8. Abundance of bioaerosol, mineral dust and fly ash in the atmosphere constructed
3 using emissions estimates in Table 3 A: Highest estimate for bioaerosol coupled to lowest
4 estimates for dust and fly ash. B: Lowest estimate of bioaerosol in the atmosphere coupled to
5 highest estimates for dust and fly ash. C and D: Effect of misidentification of phosphate- and
6 organic nitrogen-containing aerosol as biological using the emissions in A and B,
7 respectively. The hatched regions correspond to the misidentified fractions of mineral dust
8 and fly ash. In these estimates the correct emissions (solid green region) in A and B (17 and
9 2%, respectively) are overestimated (hatched green region of misidentified aerosol plus solid
10 green region) in C and D (as 81 and 77%, respectively).



1

2 Figure 9. Exemplary PALMS negative polarity spectra of A: dry-dispersed illite NX, B: wet-
3 dispersed illite NX from a distilled, deionized water slurry and C: similarly wet-dispersed
4 illite NX but from a water slurry that also contained *F. solani* spores. Note that phosphate
5 features are absent in A and B but present in C due to addition of biological material to the
6 mineral dust.